Article

"Supramolecular" Assembly of Gold Nanorods End-Terminated with Polymer "Pom-Poms": Effect of Pom-Pom Structure on the Association Modes

Nie, Daniele Fava, Michael Rubinstein, and Eugenia Kumacheva

J. Am. Chem. Soc., **2008**, 130 (11), 3683-3689 • DOI: 10.1021/ja711150k

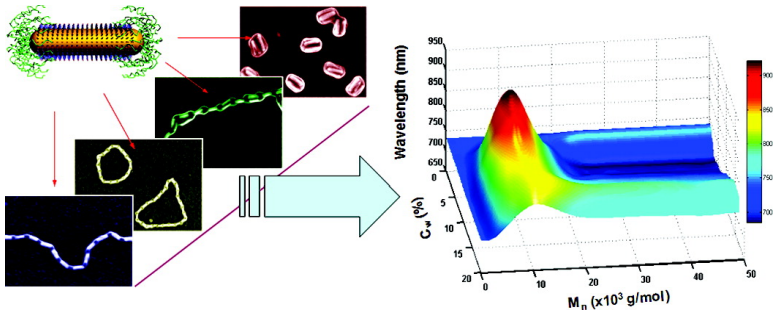

More About This Article

Additional resources and features associated with this article are available within the HTML version:

- Supporting Information
- Links to the 4 articles that cite this article, as of the time of this article download
- Access to high resolution figures
- Links to articles and content related to this article
- Copyright permission to reproduce figures and/or text from this article

View the Full Text HTML

J|A|C|S
ARTICLES
Published on Web 02/26/2008

"Supramolecular" Assembly of Gold Nanorods End-Terminated with Polymer "Pom-Poms": Effect of Pom-Pom Structure on the Association Modes

Zhihong Nie,[†] Daniele Fava,[†] Michael Rubinstein,[‡] and Eugenia Kumacheva*[,†,§,||]

Department of Chemistry, University of Toronto, 80 St. George Street, Toronto, Ontario M5S 3H6, Canada, Department of Chemistry, University of North Carolina, Chapel Hill, North Carolina 27599-3290, Institute of Biomaterials and Biomedical Engineering, University of Toronto, 4 Taddle Creek Road, Toronto, Ontario M5S 3G9, Canada, and Department of Chemical Engineering and Applied Chemistry, University of Toronto, 200 College Street, Toronto, Ontario M5S 3E5, Canada

Received December 16, 2007; E-mail: ekumache@chem.utoronto.ca

Abstract: We report a predefined self-organization of gold nanorods (NRs) end-terminated with multiple polymer arms ("pom-poms") in higher-order structures. The assembly of polymer-tethered NRs was controlled by changing the structure of the polymer pom-poms. We show that the variation in the molecular weight of the polymer molecules and their relative location with respect to the long side of the NRs resulted in two competing association modes of the nanorods, that is, their side-by-side and end-to-end assembly, and produced bundles, chains, rings, and bundled chains of the NRs. The superposition of the two variables controlling the organization of NRs allowed us to create a map showing the variation in the longitudinal plasmonic bands of the NRs achieved by their self-assembly.

Introduction

Recently, a great number of publications have reported the synthesis and fabrication of nanoparticles comprising either inorganic and organic constituents or several distinct inorganic components.[1−8] The chemical heterogeneity of the nanoparticles allowed their organization in complex, predictable structures by the use of preferential interactions between specific nanoparticle constituents and by the production of energetically favorable structures.[9] The self-assembly strategies employed conceptual similarity between multicomponent nanoparticles and their molecular analogues such as liquid crystals, surfactants, or block copolymers.[9−14] Several striking examples of "supramolecular" organization have been demonstrated, e.g., the self-assembly of Janus nanoparticles or nanoparticles tethered with amphiphilic block copolymers.[12,15]

The organization of multicomponent nanoparticles with asymmetric shapes such as metal and semiconductor nanorods (NRs) brought directionality to the self-assembled structures and allowed for the coupling of their size- and shape-dependent optical and electronic properties, e.g., band gap, absorption, emission, and conductivity.[16−19] The tethering of inorganic NRs with organic molecules led to nanoparticle organization in a broad range of structures by using chemical or physical binding of the organic tethers.[20−24] These strategies favorably comple-

[†] Department of Chemistry, University of Toronto.
[‡] University of North Carolina.
[§] Institute of Biomaterials and Biomedical Engineering, University of Toronto.
[||] Department of Chemical Engineering and Applied Chemistry, University of Toronto.

(1) Robinson, R. D.; Sadtler, B.; Demchenko, D. O.; Erdonmez, C. K.; Wang, L. W.; Alivisatos, A. P. *Science* **2007**, *317*, 355−358.
(2) Mokari, T.; Rothenberg, E.; Popov, I.; Costi, R.; Banin, U. *Science* **2004**, *304*, 1787−1790.
(3) Cozzoli, P. D.; Pellegrino, T.; Manna, L. *Chem. Soc. Rev.* **2006**, *35*, 1195−1208.
(4) Hurst, S. J.; Payne, E. K.; Qin, L. D.; Mirkin, C. A. *Angew. Chem., Int. Ed.* **2006**, *45*, 2672−2692.
(5) Kwon, K. W.; Shim, M. *J. Am. Chem. Soc.* **2005**, *127*, 10269−10275.
(6) Shi, W. L.; Zeng, H.; Sahoo, Y.; Ohulchanskyy, T. Y.; Ding, Y.; Wang, Z. L.; Swihart, M.; Prasad, P. N. *Nano Lett.* **2006**, *6*, 875−881.
(7) Gu, H. W.; Yang, Z. M.; Gao, J. H.; Chang, C. K.; Xu, B. *J. Am. Chem. Soc.* **2005**, *127*, 34−35.
(8) Gu, H. W.; Zheng, R. K.; Zhang, X. X.; Xu, B. *J. Am. Chem. Soc.* **2004**, *126*, 5664−5665.
(9) Glotzer, S. C.; Solomon, M. J. *Nat. Mater.* **2007**, *6*, 557−562.
(10) Park, S.; Lim, J. H.; Chung, S. W.; Mirkin, C. A. *Science* **2004**, *303*, 348−351.
(11) Nie, Z. H.; Fava, D.; Kumacheva, E.; Zou, S.; Walker, G. C.; Rubinstein, M. *Nat. Mater.* **2007**, *6*, 609−614.
(12) Zubarev, E. R.; Xu, J.; Sayyad, A.; Gibson, J. D. *J. Am. Chem. Soc.* **2006**, *128*, 15098−15099.
(13) Horsch, M. A.; Zhang, Z.; Glotzer, S. C. *Nano Lett.* **2006**, *6*, 2406−2413.
(14) Horsch, M. A.; Zhang, Z. L.; Glotzer, S. C. *Phys. Rev. Lett.* **2005**, *95*, 056105.
(15) Lattuada, M.; Hatton, T. A. *J. Am. Chem. Soc.* **2007**, *129*, 12878−12889.
(16) Murphy, C. J.; Gole, A. M.; Hunyadi, S. E.; Orendorff, C. J. *Inorg. Chem.* **2006**, *45*, 7544−7554.
(17) Perez-Juste, J.; Pastoriza-Santos, I.; Liz-Marzan, L. M.; Mulvaney, P. *Coord. Chem. Rev.* **2005**, *249*, 1870−1901.
(18) Hu, J. T.; Li, L. S.; Yang, W. D.; Manna, L.; Wang, L. W.; Alivisatos, A. P. *Science* **2001**, *292*, 2060−2063.
(19) Huynh, W. U.; Dittmer, J. J.; Alivisatos, A. P. *Science* **2002**, *295*, 2425−2427.
(20) Sudeep, P. K.; Joseph, S. T. S.; Thomas, K. G. *J. Am. Chem. Soc.* **2005**, *127*, 6516−6517.
(21) Joseph, S. T. S.; Ipe, B. I.; Pramod, P.; Thomas, K. G. *J. Phys. Chem. B* **2006**, *110*, 150−157.
(22) Caswell, K. K.; Wilson, J. N.; Bunz, U. H. F.; Murphy, C. J. *J. Am. Chem. Soc.* **2003**, *125*, 13914−13915.
(23) Chang, J. Y.; Wu, H. M.; Chen, H.; Ling, Y. C.; Tan, W. H. *Chem. Commun.* **2005**, *8*, 1092−1094.
(24) Salant, A.; Amitay-Sadovsky, E.; Banin, U. *J. Am. Chem. Soc.* **2006**, *128*, 10006−10007.

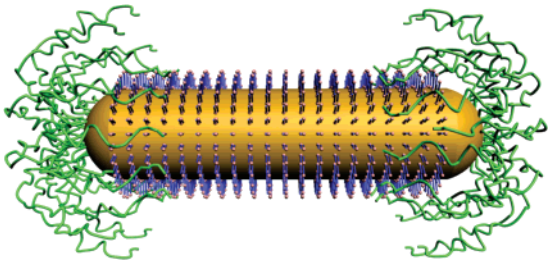

Figure 1. Schematic of the model pom-pom ABA triblock copolymer comprising a gold NR stabilized with a bilayer of CTAB and tethered at both ends with polystyrene molecules. The schematic is not to scale.

mented other methods of NR organization, e.g., the use of templates and external fields.[25−29]

Recently, we proposed a block copolymer approach to the self-assembly of inorganic NRs terminated with polymer molecules at both ends (illustrated in Figure 1).[11] The strategy for the organization of these building blocks originated from their striking resemblance to "pom-pom" ABA triblock copolymers in which two blocks comprising multiple arms are linked to a linear polymer block.[30] The self-assembly of nanorod−polymer structural units (later in the text referred to as "triblocks") was triggered by changing the selectivity of solvents for the hydrophilic central inorganic block and the hydrophobic polymer end blocks.[11]

To the best of our knowledge, the control of the self-organization of pom-pom triblock copolymers by changing their structure has not been reported; however, the self-assembly of amphiphilic oligomers comprising a rigid segment end-terminated with flexible molecules has been manipulated by varying the type and the length of the pom-pom molecules.[31−34] For example, amphiphilic dumbbell-shaped molecules were organized into spherical or toroidal micelles or planar network structures by varying the architecture of the dendron blocks attached to the central rigid segment.[32−34]

In the present paper, we report the effect of the structure of the polymer pom-poms on the organization of polymer-tethered gold NRs in the range of supramolecular structures. The structure of the polymer blocks was controlled by varying their molecular weight and the quality of solvent for the polymer molecules. The supramolecular assembly was governed by the competition between the end-to-end and side-by-side association of polymer-terminated NRs and resulted in the controlled variation of the plasmonic properties of NRs, reflected in a 3D plasmonic graph.

Results and Discussion

We used gold NRs coated with a bilayer of cetyl trimethylammonium bromide (CTAB) and end-terminated with polystyrene molecules. Gold NRs with the respective mean length and diameter of 40 ± 2 nm and 10 ± 2 nm were prepared by following the procedure of Nikoobakht and El-Sayed[35] that was scaled up to obtain a 100 mL dispersion of the nanorods (see the Supporting Information). Thiol-terminated polystyrene (PS−SH) molecules with the number-average molecular weights of 5000, 12 000, 20 000, 30 000, and 50 000 (later in the text referred to as PS-5K, PS-12K, PS-20K, PS-30K, and PS-50K, respectively) were synthesized by anionic polymerization.[36] Preferential binding of CTAB along the {100} facet of the longitudinal side of the NRs left their ends (the {111} facets) deprived of CTAB and allowed for the binding of PS−SH ligands to the ends of NRs.[22] Using the method described elsewhere,[11] we estimated the number of PS molecules grafted to each end of the NRs to be 30, 22, 19, 17, and 14 for PS-5K, PS-12K, PS-20K, PS-30K, and PS-50K, respectively. We also verified that in the triblock solution in dimethyl formamide (DMF), polymer chains form brushes at the ends of NRs (see the Supporting Information, Table S1).[37,38] Polymer-terminated NRs were readily dispersed in DMF, a good solvent for both CTAB-stabilized block and PS molecules (the second virial coefficient, A_2 of PS−DMF, and Flory−Huggins interaction parameters, χ, are 3.5×10^{-4} mol cm^3 g^{-2} and 0.46, respectively).[39−41]

The self-assembly was triggered by adding water to the solution of triblocks in DMF. To avoid the fast aggregation of triblocks, DMF/water mixture was added dropwise into the solution of triblocks in DMF. The concentration of nanorods in the DMF/water mixture was ca. 0.0075 mg·mL^{-1}. Following the addition of water, the mixture became a poor solvent for the PS blocks but remained a good solvent for the hydrophilic CTAB-stabilized metal blocks. The reducing quality of solvent for the PS constituent caused triblock association: the binding of the polymer molecules of the neighboring NRs reduced the surface energy of the system.[11,42]

In the first series of experiments, we examined the effect of the molecular weight of PS on the self-assembly of triblocks in DMF/water mixtures with a fixed concentration of water, C_W = 6 wt %. Figure 2 (left column) shows the schematics of the polymer pom-pom at the NR end. The starlike structure of the pom-pom polymer block allowed PS chains to form a corona around the ends of the NRs, with a fraction of PS chains spreading along the longitudinal side of the NRs.[43] With increasing molecular weight of PS (that is, with increasing length of PS molecules), the extent of coverage of the longitudinal side of the metal block by polymer chains increased. The central and the right columns in Figure 2 show the schematics of

(25) Khanal, B. P.; Zubarev, E. R. *Angew. Chem., Int. Ed.* **2007**, *46*, 2195−2198.
(26) Correa-Duarte, M. A.; Perez-Juste, J.; Sanchez-Iglesias, A.; Giersig, M.; Liz-Marzan, L. M. *Angew. Chem., Int. Ed.* **2005**, *44*, 4375−4378.
(27) Zhang, Q. L.; Gupta, S.; Emrick, T.; Russell, T. P. *J. Am. Chem. Soc.* **2006**, *128*, 3898−3899.
(28) Ryan, K. M.; Mastroianni, A.; Stancil, K. A.; Liu, H. T.; Alivisatos, A. P. *Nano Lett.* **2006**, *6*, 1479−1482.
(29) Dujardin, E.; Hsin, L. B.; Wang, C. R. C.; Mann, S. *Chem. Commun.* **2001**, *14*, 1264−1265.
(30) Knauss, D. M.; Huang, T. Z. *Macromolecules* **2002**, *35*, 2055−2062.
(31) Bae, J.; Choi, J. H.; Yoo, Y. S.; Oh, N. K.; Kim, B. S.; Lee, M. *J. Am. Chem. Soc.* **2005**, *127*, 9668−9669.
(32) Lee, J.; Jeong, Y. H.; Kim, J. K.; Lee, M. *Macromolecules* **2007**, *40*, 8355−8360.
(33) Kim, J. K.; Lee, E.; Huang, Z. G.; Lee, M. *J. Am. Chem. Soc.* **2006**, *128*, 14022−14023.
(34) Kim, J. K.; Lee, E.; Jeong, Y. H.; Lee, J. K.; Zin, W. C.; Lee, M. *J. Am. Chem. Soc.* **2007**, *129*, 6082−6083.
(35) Nikoobakht, B.; El-Sayed, M. A. *Chem. Mater.* **2003**, *15*, 1957−1962.
(36) Stouffer, J. M.; McCarthy, T. J. *Macromolecules* **1988**, *21*, 1204−1208.
(37) Degennes, P. G. *Adv. Colloid Interface Sci.* **1987**, *27*, 189−209.
(38) Milner, S. T. *Science* **1991**, *251*, 905−914.
(39) Wolf, B. A.; Willms, M. M. *Makromol. Chem.* **1978**, *179*, 2265−2277.
(40) Schulz, G. V.; Baumann, H. *Makromol. Chem.* **1968**, *114*, 122−138.
(41) Rubinstein, M.; Colby, R. H. *Polymer Physics*; Oxford University Press: Oxford, 2003.
(42) Israelachvili, J. N. *Intermolecular and surface forces*; Academic Press: London, 1992.
(43) In the control experiments, partial wetting of the CTAB-coated gold surface with polystyrene chains was confirmed by atomic force microscopy imaging of CTAB-coated planar gold surfaces exposed to the solution of nonfunctionalized polystyrene in DMF.

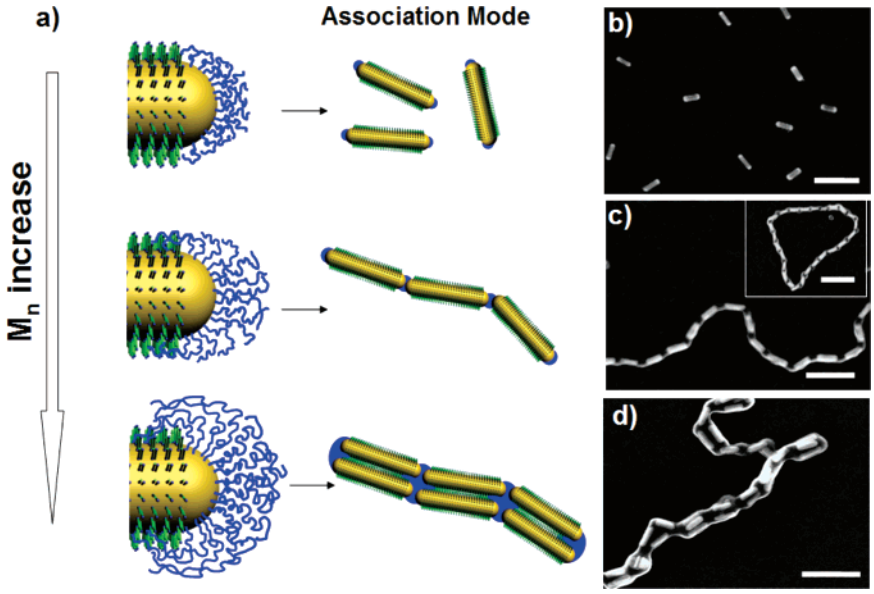

Figure 2. Left column: Schematics of the relative location of PS molecules with varying molecular weight with respect to the central gold block. Central column: Schematics of the self-assembled structures of triblocks when water is added to the solution of NRs in DMF. The schematics are not to scale. Right column: scanning electron microscopy (SEM) images of the self-assembled structures of triblocks carrying PS-5K (b), PS-12K (c), and PS-30K (d) in a water/DMF mixture with 6 wt % water. Scale bar is 100 nm.

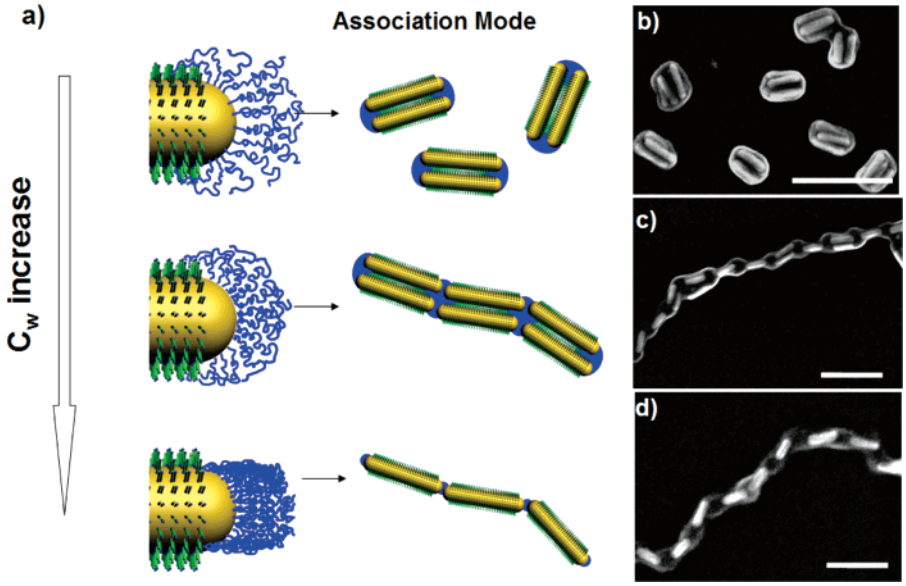

Figure 3. Left column: Schematics of the relative location of PS molecules with respect to the central gold block in water/DMF mixtures with varying water content. Central column: Schematics of the self-assembled structures of triblocks with 50K-PS. The schematics are not to scale. Right column: SEM images of corresponding assembled structures of triblocks with 50K-PS in water/DMF mixture with 4 wt % water (b), 10 wt % water (c), and 20 w% water (d). Scale bar is 100 nm.

association modes and the experimentally observed self-assembled structures of triblocks, respectively. For short PS molecules (PS-5K) no self-assembly of triblocks occurred, whereas with increasing molecular weight of PS the triblocks organized into chains. Under particular conditions (see below) the chains of triblocks formed rings. Further increase in the coverage of the long side of the NR block with PS molecules led to both end-to-end and side-by-side assembly of triblocks and the formation of bundled chains.

In the second series of experiments, we varied the fraction of water, C_W, in the solution of NRs end-terminated with PS molecules with a particular molecular weight. Figure 3 (left column) shows that with increasing amount of water added to the solution of NRs in DMF, the PS molecules relocated from the long faces of the NRs to their edges. The change in the relative location of PS molecules reduced the energy of the PS−solvent interface and decreased the energy of the CTAB−solvent interface. The resulting association modes of triblocks and experimentally observed structures are shown in the middle and right columns, respectively, in Figure 3.

The results of the systematic study of the self-assembly of triblocks are presented as a phase diagram (Figure 4). For $C_W < 3$ wt %, the triblocks carrying PS molecules with different molecular weights exist as individual entities: the energy gain due to the linkage of PS chains of the neighboring nanorods was insufficiently high for the entropy loss due to triblock association. At the content of water of 4 wt %, the triblocks carrying PS-5K remained nonaggregated; however the triblocks

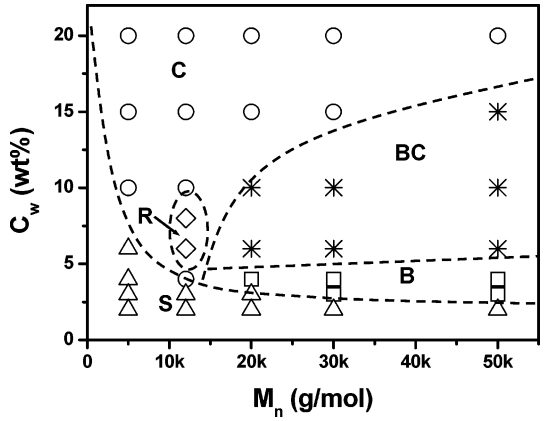

Figure 4. Phase diagram of the self-assembly of metal−polymer triblocks with varying length of hydrophobic blocks in water/DMF mixtures. Key: S, single NRs; R, rings with chains; C, chains; B, bundles; BC, bundled chains. The established morphological boundaries (dashed lines) do not reflect precise transition conditions. The concentration of nanorods in the DMF/water mixture was ca. 0.0075 mg·mL^{-1}.

comprising PS-12K assembled in the nanochains by connecting two PS ends (Figure 2c). The triblocks with polystyrene blocks of larger molecular weights (PS-20K, PS-30K, and PS-50K) showed preferential side-by-side assembly in bundles (Figure 3b). We explain the formation of bundles, instead of chains or bundled chains, by the repulsion between PS molecules squeezed against each other in the central part of the polymer corona. Because of the small spacing between these high-molecular-weight PS molecules, the three-body repulsion between their chains was stronger than the two-body attraction.[41] (The characteristics of PS molecules grafted to the edges of NRs are provided in the Supporting Information.) Hence, upon the end-to-end approach of triblocks, PS brushes in the central part of the corona repelled each other. By contrast, PS molecules attached to the periphery of the NR edges were not squeezed against each other, and the two-body attraction was stronger than the three-body repulsion,[41] causing adherence between these sections of triblocks and leading to their side-by-side assembly. We note that the side-by-side association of NRs did not occur for the nanorods carrying PS blocks with low molecular weight (PS-5K and PS-12K) because of the short length of polymer molecules.

For 6 wt % $\leq C_W \leq$ 8 wt %, a large fraction (up to ca. 50%) of the triblocks carrying PS-12K formed rings (shown in inset in Figure 2c) by the enclosure of the linear nanochains. For triblocks comprising PS molecules with higher molecular weights, the polymer pom-pom partly spread over the long facet of the NR block and at $C_W \geq$6 wt % the combined side-by-side and end-to-end association of triblocks yielded bundled chains (shown in Figures 2d and 3c). The bundled chains were rigid and did not favor the formation of rings, due to the high energy cost of the bending of stiff chains. With increasing C_W, the hydrophobic polymer chains were pulled away from the longitudinal facet of the NRs to the region between the ends of the NRs, in order to reduce the total interfacial energy between the three phases of solvent, polystyrene, and CTAB. Therefore, for $C_W \geq$ 15%, the difference in the self-assembly of NRs carrying PS molecules with different molecular weights was removed: because of the reorganization of the PS molecules and a large unfavorable interaction of PS with the solvent, all triblocks underwent end-by-end self-assembly in chains comprising a single NR in the cross-section (Figure 3d).

Furthermore, to examine the competition between the side-by-side and end-to-end assembly modes of triblocks, we determined the average side-by-side and end-to-end aggregation numbers, N_{s-s} and N_{e-e}, respectively, that were characteristic for the types of structures observed in the present work. To find N_{s-s} we used the equation $N_{s-s} = (\sum_{i=1}^{\infty} n_i N_i / \sum_{i=1}^{\infty} n_i)$ where n_i is the number of aggregates in which N_i triblocks assembled side-by-side. (In the case of bundled chains, we counted N_i for n_i fragments with the length of one triblock in the direction of the long axis of each chain.) The values of N_{e-e} were found as $N_{e-e} = (\sum_{i=1}^{\infty} n_i / X)$ where X is the number of chains. Figure 5a shows the variation in N_{s-s} and N_{e-e} as a function of the molecular weight of PS for C_W = 6 wt %. The value of N_{s-s} increased and the value of N_{e-e} decreased with the molecular weight of PS increasing from 12 000 to 50 000. (For PS-5K, no end-to-end or side-by-side self-assembly occurred, yielding values of both N_{s-s} and N_{e-e} equal to 1.) Figure 5b shows the effect of the concentration of water in the DMF/water mixture on the variation in N_{s-s} and N_{e-e} for PS-50K. With increasing concentration of water, N_{s-s} decreased from ca. 2.8 to ca. 1.1 and N_{e-e} increased from ca. 2 to ca. 38. Overall, a strong anticorrelation of side-by-side and end-to-end aggregation was observed: the factors that favored end-to-end self-assembly reduced the number of triblocks associated side-by-side. We note that the side-by-side assembly of triblocks dominated only in a very narrow range of water content ($C_W \sim$ 3−4 wt %). At higher values of C_W, the aspect ratio of the self-assembled structures increased and the end-to-end assembly made NRs dominated chains.

Furthermore, since the distance between the metal blocks organized in the chains determines the extent of coupling of plasmonic properties of the NRs, we examined the effect of molecular weight of PS molecules on the distance between the ends of adjacent NRs. Images in Figure 6a−c show a notable increase in the spacing between the nanorods end-tethered with PS molecules with varying molecular weights and organized in chains. Figure 6d shows that the average end-to-end distance, D, between the neighboring NRs increased with molecular weight of PS, due to the increase in the amount of the polymer confined between the ends of NRs. The distance, D, between the ends of NRs increased at higher water content, due to the relocation of PS molecules from the longitudinal facets to the space between adjacent NRs. The conformation of PS molecules between the NR ends was characterized as the variation in $D/(2\langle R_0 \rangle)$ with $\langle R_0 \rangle$ (Figure 6e) where $\langle R_0 \rangle$ is the estimated mean-square end-to-end distance of the PS chain ($\langle R_0 \rangle = bN^{1/2}$ where b is the Kuhn length (b = 18 Å for polystyrene), N is the number of Kuhns segments of length b,[41] and factor 2 in $D/(2\langle R_0 \rangle)$ is used because the distance D includes PS from two ends of the NRs). In Figure 6e, the values of $D/(2\langle R_0 \rangle) < 1.15$ indicate that in the self-assembled triblock chains the PS molecules at the ends of NRs were in the collapsed state partly because of decreasing grafting density of polystyrene molecules.[41]

Finally, we examined the effect of the structure of PS pom-poms on the variation in the plasmonic properties of self-assembled NRs. On the basis of the results of SEM and TEM imaging (Figures 2 and 3; also see the Supporting Information, Figures S1 and S2) and earlier theoretical and experimental

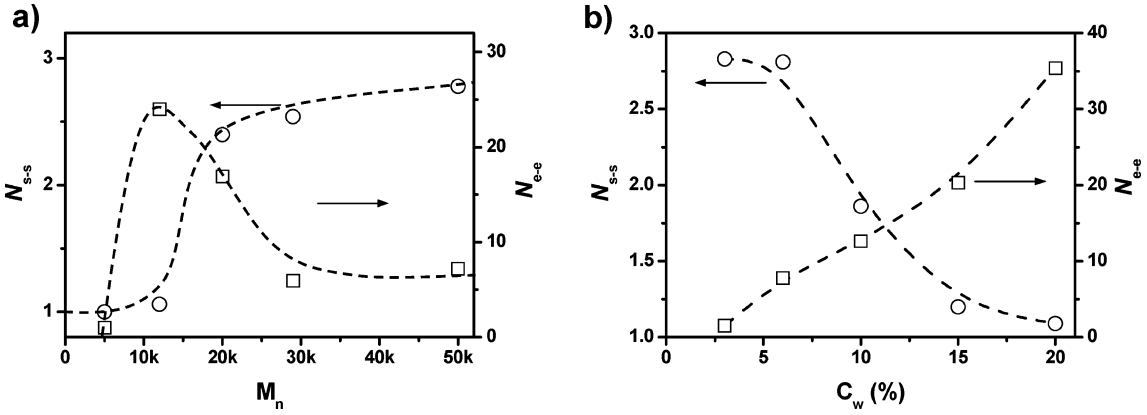

Figure 5. (a,b). Variation in the average aggregation numbers, N_{s-s} and N_{e-e}, characteristic for the side-by-side and end-to-end association of triblocks, respectively, plotted as (a) a function of the molecular weight of PS in the DMF/water mixture at C_W = 6 wt % and (b) a function of the concentration of water concentration in the DMF/water mixture for the NRs end-terminated with PS-50K.

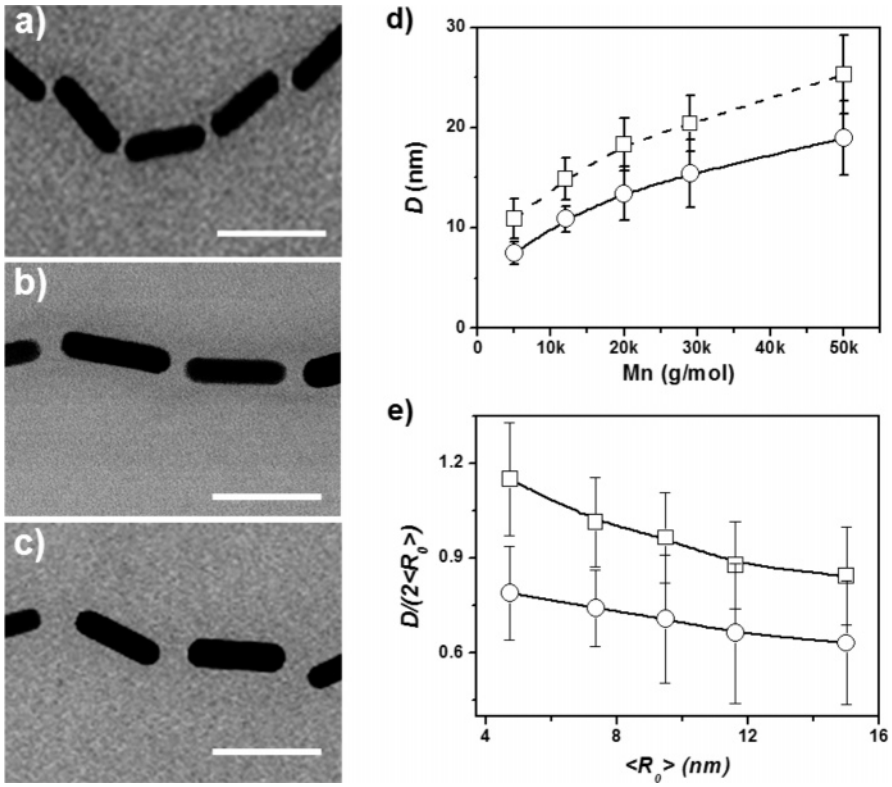

Figure 6. (a−c) Transmission electron microscopy (TEM) images of self-assembled nanochains of nanorods end-terminated with PS-5K (a), PS-12K (b), and PS-50K (c) in a water/DMF mixture with C_W = 15%. Scale bar is 50 nm. (d) Variation of the average end-to-end distance between adjacent NRs of assembled chains, D, at C_W = 15% (○) and 20% (□) plotted as a function of number-average molar mass of PS. The values of D were found by image analysis of the TEM images. (e) Variation of the distance, D, normalized by mean-square end-to-end distance of PS, $D/(2\langle R_0\rangle)$ at C_W = 15% (○) and 20% (□) plotted as a function of mean-square end-to-end distance, $\langle R_0\rangle$, of PS chains.

findings,[44,45] we expected to observe a blue shift in the longitudinal plasmonic band of the NRs assembled side-by-side and a red shift in the longitudinal plasmonic band of the end-to-end assembled NRs. Both shifts were attributed to the coupling of the plasmons of the two interacting neighboring NRs. Figure 7a,b shows representative spectra of the NRs end-terminated with PS-5K and PS-50K, respectively. In both graphs, the vertical dotted line shows the spectral position of the individual polymer-tethered NRs in the DMF solution. In Figure 7a, a longitudinal plasmonic band of the NRs stabilized with PS-5K at water content values of 4 and 6 wt % showed an insignificant shift indicating that the triblocks existed as individual species (the shift of ca. 2 nm occurred due to the change in dielectric constant of the solvent). At C_W > 10 wt %, the spectrum of the same triblocks featured a 35 nm red shift of the longitudinal plasmonic band, confirming the formation of chains. For triblocks with PS-12K, the red shift of the longitudinal plasmonic band was as large as ca. 180 nm, because of the formation of long chains of NRs (see the Supporting Information, Figure S3). The extent of red shift decreased with increasing values of C_W, owing to the increasing distance between the ends of NRs organized in chains. The side-by-side assembly of NRs bearing PS-50K at C_W values of 4

(44) Jain, P. K.; Eustis, S.; El-Sayed, M. A. *J. Phys. Chem. B* **2006**, *110*, 18243−18253.
(45) Su, K. H.; Wei, Q. H.; Zhang, X.; Mock, J. J.; Smith, D. R.; Schultz, S. *Nano Lett.* **2003**, *3*, 1087−1090.

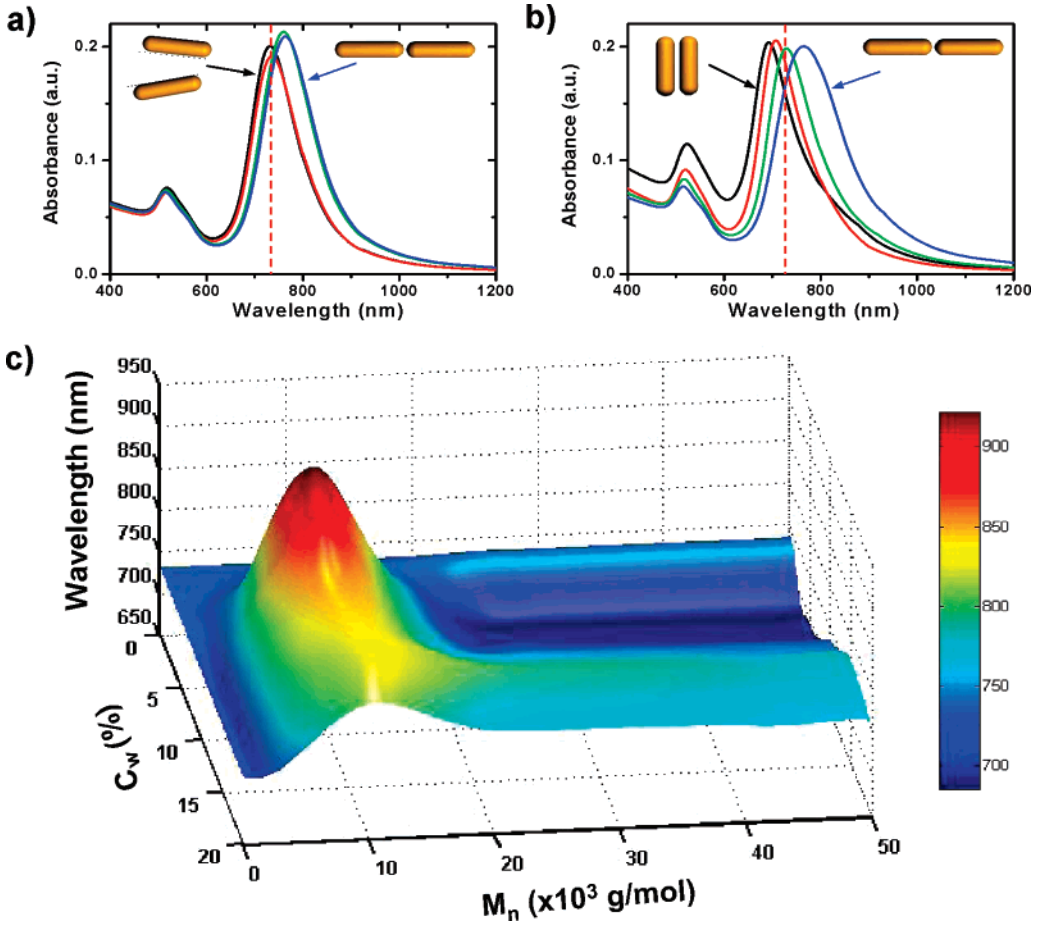

Figure 7. (a,b) UV−vis spectra of self-assembled triblocks carrying PS-5K (a) and PS-50K (b) in the DMF/water mixtures with C_W values of 4 wt % (black), 6 wt % (red), 10 wt % (green), and 15 wt % (blue). Vertical dashed lines show the spectral positions of the longitudinal plasmonic band of the individual PS-tethered NRs in DMF solution. (c) Variation in the longitudinal plasmonic bands of self-assembled nanorods plotted on the (M_n, C_W) space. Color in the graph represents the wavelengths of the longitudinal plasmonic band. The longitudinal plasmonic band of the individual NRs is 731 nm.

and 6% resulted in a 40 and 25 nm blue shift of the longitudinal plasma band, respectively (Figure 7b), corresponding to the formation of bundles and short bundled chains. We also observed up to a ~10 nm red shift in the transverse plasma band (see the Supporting Information, Figure S4), for the side-by-side assembled NRs, due to the transition of the dipolar exciton to the lower-energy excited state, in agreement with the previous report by El-Sayed et al.[44] With increasing water content, the longitudinal plasma band of triblocks carrying PS-50K shifted toward long wavelengths because the end-to-end assembly was favored at high water content (Figure 7b).

To summarize, the shifts in the longitudinal plasmonic bands (governed by the side-by-side or end-to-end assembly of the NRs) were controlled by the molecular weight of PS molecules and/or the value of C_W. Figure 7c presents a 3D graph in which the wavelengths of the longitudinal plasmonic bands of the self-assembled NRs are plotted as a function of the molecular weight of PS and C_W. This graph provides guidance in tuning the plasmonic properties of gold NRs by their controlled self-organization.

In conclusion, we showed that in the DMF/water mixtures, the self-assembly of NRs end-terminated with PS molecules originates from the pom-pom structure of the polymer blocks and is determined by the length and distribution of PS molecules between the ends of NRs and the longitudinal facet of NRs. Following the relocation of the polymer molecules from the long facet to the end of the metal blocks, the assembly of nanorods underwent the following transitions: bundles → bundled chains → chains. The transitions were controlled by two anticorrelating parameters: the molecular weight of the polymer tethered to NR ends and the concentration of water in the system. The predetermined assembly of polymer-tethered NRs may prove useful in the fabrication of functional devices. For example, the organization of NRs in chains, that is, preferential alignment parallel to the axis of the structure, may find applications in the fabrication of plasmon waveguides and switches for integrated nanoscale optics.[46]

Acknowledgment. The authors thank NSERC Canada for financial support of this work under the Discovery and Canada Research Chair program. M.R. acknowledges the financial support of the National Science Foundation under Grants CHE-0616925 and CTS-0609087 and the National Institutes of Health under Grant 1-R01-HL0775486A. We thank Professor Gilbert C. Walker for useful discussions.

Supporting Information Available: Description of the synthesis and surface modification of gold nanorods; description

(46) Maier, S. A.; Brongersma, M. L.; Kik, P. G.; Meltzer, S.; Requicha, A. A. G.; Atwater, H. A. *Adv. Mater.* **2001**, *13*, 1501−1505.

of the self-assembly experiments; estimation of the number of PS chains on the ends of NRs and the evaluation of polymer brush state; TEM images of the self-assembled structures; absorption spectra of the self-assembled NRs; and results of dynamic light scattering experiments. This material is available free of charge via the Internet at http://pubs.acs.org.

JA711150K